DOI: 10.1002/ange.200704861

Silver in Zeolites

Photoactivation of Silver-Exchanged Zeolite A**

*Gert De Cremer, Yasuko Antoku, Maarten B. J. Roeffaers, Michel Sliwa, Jasper Van Noyen, Steve Smout, Johan Hofkens, Dirk E. De Vos, Bert F. Sels, and Tom Vosch**

Clusters of silver atoms and ions have attracted the interest of scientists because of their pronounced catalytic[1] and emissive properties.[2] To prevent aggregation of the clusters into larger particles, stabilization in gas matrices at cryogenic temperatures,[3] or in scaffolds such as polyphosphates,[4,5] DNA,[2,6] peptides[7] or polymers[8] at ambient temperature, has been suggested.

Alternatively, zeolites have been proposed to stabilize small ionic silver clusters.[9–12] The molecular dimensions of the zeolite cages and channels prevent aggregation into larger nanoparticles (because of steric reasons) while the net negative charge of the zeolite lattice, the coordinating properties of the lattice oxygen atoms, and the presence of additional cations play a crucial role in stabilizing cationic clusters and unstable intermediates during reduction. Reduction of silver in zeolites is usually a bulk process that requires reductants, such as hydrogen gas or sodium borohydride, but also γ irradiation[4] and visible light[13] can cause reduction. One of the most studied systems is silver-exchanged zeolite A (LTA topology), and several models have been proposed to explain the nature and location of the silver clusters formed in this zeolite upon reduction.[14]

Aside from their catalytic properties, oligonuclear silver clusters show particularly bright and stable luminescent properties.[2] However, the existing fluorescence studies about Ag clusters in zeolites are limited to the excitation and emission spectra of bulk powder samples.[10,15] Here, we report on bright fluorescent (spots in) individual silver-exchanged zeolite 3A crystals obtained upon photoactivation using a focused UV irradiation on a fluorescence microscope. Photoactivation of silver has been demonstrated for nanoscale Ag_2O particles (and interpreted as a photoreduction process).[13] In our study, the emissive silver material is confined within a zeolite framework, which results in a better control of the type and location of the emissive species formed upon UV irradiation. Silver-cluster-loaded crystals are technologically very attractive—for example, as secondary light sources in fluorescence lamps—because of their high emission intensity, their excellent photostability upon UV irradiation, and their large Stokes shift.[16,17] Moreover, the space-resolved selective activation of the emission intensity may have important applications in data storage.

The emissive zeolite particles used herein were prepared by exchanging zeolite 3A with (8 ± 1) wt % Ag^+ (from $AgNO_3$ solutions), followed by heating for one day at 450 °C (see the Supporting Information). The enhanced emission exhibited by the silver-exchanged zeolites after the thermal treatment has been ascribed to two possible causes: 1) to the formation of charge-transfer complexes between the partially (de)hydrated silver ions and the oxygen atoms in the zeolite lattice[11,16,17] or 2) to the emissive properties of autoreduced oligoatomic silver clusters that may be formed during the high-temperature treatment.[9] Although this report focuses on the photoactivation of thermally treated Ag zeolites, control experiments performed on not thermally activated Ag zeolites (dried at 110 °C) show an analogous photoactivation behavior (see the supporting Information).

Figure 1 a(1), b(1) shows typical confocal scanning images of a heat-treated Ag-containing zeolite crystal (roughly $3\times3\ \mu m^2$ in size) taken under a confocal microscope using a picosecond-pulsed 375 nm excitation source (doubled Ti:Sapphire, Spectra Physics; see the Supporting Information). Figure 1 a and 1 b were taken at excitation intensities of 10 and 20 $W\,cm^{-2}$, respectively. Zeolite crystals that were not treated thermally exhibited an emission ten-times-weaker than that of the thermally treated samples.

The confocal approach in combination with the pinhole in the emission path (see the Supporting Information) allows the collection of photoemission data from selected parts inside the crystals. Diffraction-limited bright spots can be generated at specific domains inside an individual crystal by simply focusing a low-power UV laser at the target position; for instance, in the crystal shown in Figure 1 a, three individual spots were selectively activated by irradiation during

[*] Dr. Y. Antoku, Dr. M. Sliwa, S. Smout, Prof. Dr. J. Hofkens, Dr. T. Vosch
Department of Chemistry
Katholieke Universiteit Leuven
Celestijnenlaan 200F, 3001 Heverlee (Belgium)
Fax: (+32) 1632-7989
E-mail: tom.vosch@chem.kuleuven.be
G. De Cremer, M. B. J. Roeffaers, J. Van Noyen, Prof. Dr. D. E. De Vos, Prof. Dr. B. F. Sels
Department of Microbial and Molecular Systems
Katholieke Universiteit Leuven
Kasteelpark Arenberg 23, 3001 Heverlee (Belgium)
Fax: (+32) 1632-1998
E-mail: bert.sels@biw.kuleuven.be

[**] T.V. and G.D.C. acknowledge the F.W.O. (Fonds voor Wetenschappelijk Onderzoek) for a postdoctoral and a doctoral fellowship, respectively. M.B.J.R. thanks the Institute for the Promotion of Innovation through Science and Technology in Flanders (IWT-Vlaanderen) for a doctoral fellowship. This work was performed within the framework of the IAP-VI program "Supramolecular Chemistry and Catalysis" of the Belgian Federal government and of GOA-2/01. We also gratefully acknowledge support from the K.U. Leuven in the frame of the Centre of Excellence CECAT. We thank F. C. De Schryver for fruitful discussions and R. De Vos for help with the SEM measurements.

Supporting information for this article is available on the WWW under http://www.angewandte.org or from the author.

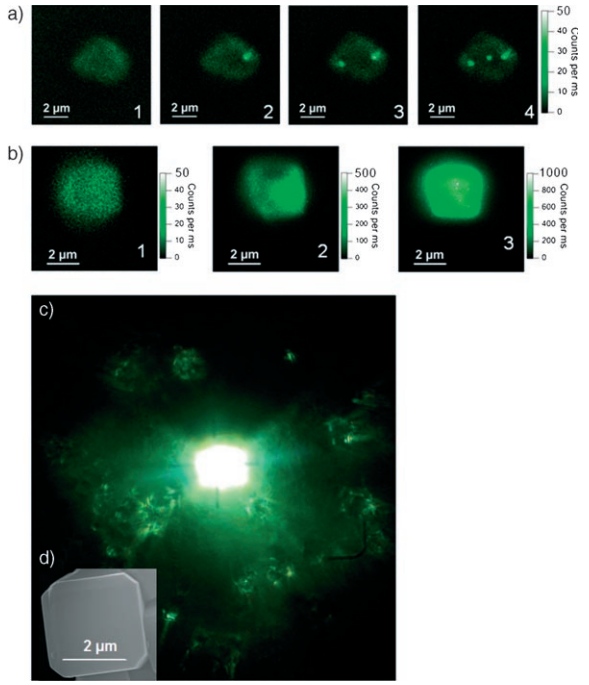

Figure 1. a) False-color emission images of an individual silver-exchanged zeolite A crystal before photoactivation (1) and after consecutive activation of three individual spots (2, 3, and 4) by irradiation (for 20 minutes) with a low-power (10 $W cm^{-2}$) picosecond-pulsed 375 nm laser through a confocal microscope (images taken at an excitation intensity of 10 $W cm^{-2}$ with a 2-ms integration time per pixel). b) Upon high-power illumination (16.7 $kW cm^{-2}$), the strong scattering of the focused excitation beam causes photoactivation of the emission throughout the whole crystal. Image (1) shows the crystal before activation. Images (2) and (3) show the same crystal after 5 and 25 minutes of high-power illumination (images taken at an excitation intensity of 20 $W cm^{-2}$ with a 2-ms integration time per pixel). c) True-color image taken with a Canon PowerShot A710 IS digital camera with a 400 nm longpass filter through the eyepiece of the microscope showing the green emission from the crystal shown in (b) after complete activation at an excitation power of 16.7 $kW cm^{-2}$. d) SEM image of characteristic silver-exchanged zeolite A crystals (see also the Supporting Information).

20 minutes with the same source at 10 $W cm^{-2}$ (panels 1 to 4). The observation of one, two or three bright individual spots illustrates the write-and-read potential of the material in data-storage applications. On the other hand, illumination with extremely high power causes strong scattering of the excitation light throughout the whole crystal. In such conditions, the complete crystal—instead of chosen domains—is activated (Figure 1b). After five minutes of UV illumination at 16.7 $kW cm^{-2}$, a tenfold increase in the emission intensity at the focal spot had been realized [see Figure 1b(2)]. After further 20 minutes of high-intensity irradiation, the emission in the crystal reached a plateau at a 20-fold intensity increase [see Figure 1b(3)]. Figure 1c shows a true-color image of the same crystal under UV excitation at 16.7 $kW cm^{-2}$ (observed through the eyepiece of the microscope). In contrast to quantum dots, which are composed of semiconductor nanocrystals,[18] the luminescence of this zeolite-based material is free of blinking, because the emission originates from multiple silver-particle emitters confined within one crystal (see the Supporting Information).

The dynamics of the activation process were monitored by recording successive emission spectra integrated over intervals of one second (or of ten seconds for the lowest excitation intensity). A plot of the maximum emission intensities of these spectra as a function of time reveals a sigmoidal behavior with characteristic lag times of up to a few hundreds of seconds at low excitation powers before the actual activation takes place (see Figure 2). A similar observation

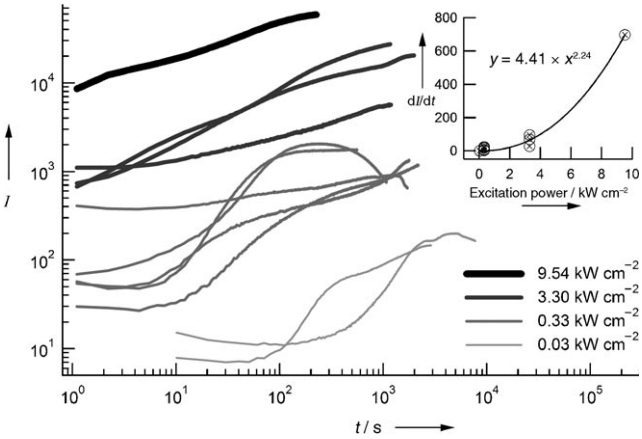

Figure 2. Bilogarithmic plot for the time evolution of the emission intensity (activation curves) of 11 different individual Ag-loaded zeolite crystals (calcined at 450 °C) excited with four different activation intensities. The inset shows a plot of the maximum activation rate (dI/dt of the linear part of the activation curves) achieved for each crystal as a function of the excitation power. These data points were fitted to a power function and show a nonlinear behavior (with an exponent of 2.2).

was made in an electron paramagnetic resonance (EPR) study of the formation of the Ag_6^+ species in an Ag,K-A zeolite upon hydrogen reduction.[19] In that work, the induction period was explained by the low mobility of the K^+ and Ag^+ ions in combination with the stepwise mechanism for the Ag_6^+ cluster formation. The occurrence of a lag time in the activation curves shown in Figure 2 suggests that the emissive species (namely, Ag_n^{m+}) also require a minimal nuclearity before they become highly emissive at this excitation wavelength.

After reaching its maximum value for a certain excitation power, the emission intensity of an irradiated spot can be further enhanced by increasing the excitation power (see the Supporting Information). The plateau behavior shown in the activation curves suggests a steady state between cluster formation and destruction rather than a full conversion of the silver species. Similar steady states between Ag-cluster creation and destruction have been proposed in photoactivation studies performed on AgO surfaces.[20] In the case of the zeolite, the equilibrium situation is stable for several hours—mostly without photobleaching. Only a few crystals exhibit a small intensity decrease after the maximum emission has been reached. Although we cannot fully exclude instrumental artefacts, this intensity decrease may result from the forma-

tion of larger nonfluorescent silver particles after prolonged irradiation.

The maximum slope in the sigmoidal activation curves shows a nonlinear relationship with the applied excitation power (Figure 2, inset). This behavior indicates the involvement of multiple photons in the formation of the activated Ag clusters (either by a simultaneous or consecutive two-photon absorption process or by the occurrence of two independent simultaneous photochemical reactions), which causes the reaction kinetics to be of a higher order with respect to the excitation intensity. A similar effect was described for the formation of silver clusters through the photochemical reduction of an AgO layer.[20]

The heterogeneity in the activation curves of Figure 2 at identical powers is characteristic of studies on individual crystals. A similar large spread of the emission intensity was observed for individual perylene-loaded zeolite crystals.[21] Heterogeneities inside a zeolite crystal—or between individual zeolite crystals in a population—are at the origin of these phenomena, and they have recently been mapped by means of fluorescence microscopy using various probes and pro-fluorescent reagents.[22]

Spectral analysis after UV activation reveals a dominant greenish emission with a distinct maximum at (540 ± 4) nm upon 375 nm excitation (Figure 3). On the other hand, the highly heterogeneous emission spectra of the loaded crystals before photoactivation showed emission maxima between 493 and 541 nm. This UV-induced red shift of the emission wavelength can only be explained by the formation of a limited number of specific cluster types, which dominate the emission spectrum.

In addition to the red shift of the emission signals, we also observed a shortening of the average fluorescence decay time during UV photoactivation using an avalanche photodiode detector (APD) in the single-photon counting experiments (see the Supporting Information). Sufficient emission intensity for a detailed emission-wavelength-dependent study of the decay times on a single zeolite crystal using a photomultiplier tube (PMT) detector with a sub-10-ps time resolution after deconvolution can only be achieved after UV photoactivation at high-power illumination (Table 1).

Table 1: Contributions and decay times of the different fluorescence-decay components for two single crystals at different emission wavelengths.[a,b]

	Crystal 1[c]			Crystal 2[d]		
λ_{em} [nm]	$\alpha_{0.12\ ns}$ [%]	$\alpha_{0.92\ ns}$ [%]	$\alpha_{3.41\ ns}$ [%]	$\alpha_{0.20\ ns}$ [%]	$\alpha_{1.26\ ns}$ [%]	$\alpha_{4.03\ ns}$ [%]
460	16.1	39.0	45.0	28.0	56.3	15.7
480	11.7	36.1	52.2	23.2	56.6	20.1
500	7.6	30.2	62.3	16.3	52.7	30.9
520	4.5	24.4	71.1	8.7	41.5	49.7
540	2.7	20.7	76.6	5.2	32.3	62.5
560	1.6	18.6	79.7	3.6	25.0	71.4
580	1.5	16.9	81.7	2.7	19.8	77.4
600	1.4	15.9	82.8	2.5	15.8	81.7
620	1.2	17.3	81.5	2.6	13.7	83.7
640	1.3	20.9	77.7	2.7	11.8	85.5

[a] Obtained by global analysis with linked τ values for all the emission wavelengths of a crystal. [b] A graphical representation of the data can be found in the Supporting Information. [c] χ^2 of the global fit = 1.039; excitation power: 1.83 kW cm^{-2}. [d] χ^2 of the global fit = 1.174; excitation power: 16.7 kW cm^{-2}.

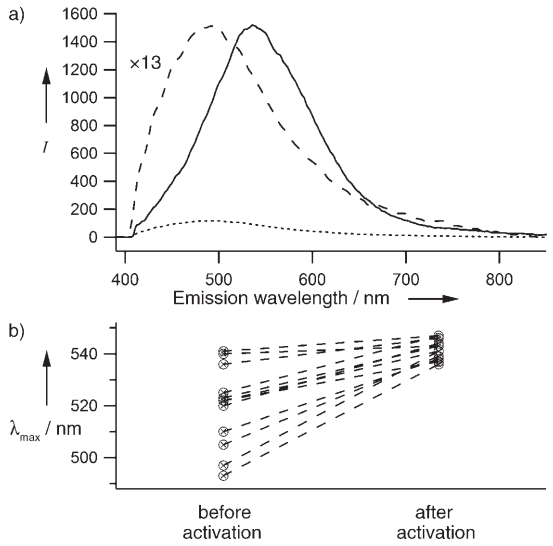

Figure 3. a) Emission spectrum before (•••••) and after (——) photoactivation for an individual crystal. The dashed line (-----) represents the spectrum before activation normalized (×13) to the maximum intensity after activation. b) Emission maxima before and after photoactivation for 11 individual crystals. The maxima are found within a broad wavelength range before activation and converge into a narrow band (at about 540 nm) after activation. All spectra were taken upon excitation with a 375 nm picosecond-pulsed laser at excitation powers between 33 and 9.5 kW cm^{-2}.

The luminescence decay shows three distinct components (of approximately 100 ps, 1 ns, and 4 ns) in the UV-activated Ag-containing 3A zeolite crystal. The obtained decays were analyzed globally and fitted with a triexponential decay function using a time-resolved fluorescence analysis (TRFA) software[23] to link the characteristic decay times, τ, for all emission wavelengths. At higher emission wavelengths, the contribution of the fast-decay component—and to a lesser extent also that of the medium-decay component—decreases in favor of the slowest decay (see the Supporting Information). Provided that the different decay times can be linked to different emissive species, the spectral characteristics will suggest the presence of different (or identical) silver nanoclusters in different local environments within the zeolite guest.

In summary, we present an in-depth microscopic characterization of the emissive properties of Ag-loaded zeolites. In contrast to common procedures, silver reduction is stimulated by UV radiation, which offers a high degree of controllability in time (ms) and space (submicron). The space-resolved photoactivation of Ag-loaded materials allows access to well-localized bright and photostable spots in a 3D crystal, which may have important applications in the development of data-storage devices. Thanks to the broad emission range and high photostability upon UV illumination, the highly emissive material may also serve as secondary light sources in

fluorescence lamps. The nonblinking emission behavior additionally opens possibilities for use as bright, photostable labels. The properties of the distinct silver clusters as well as details of the activation mechanism in relation with the zeolite composition are currently being studied.

Received: October 19, 2007
Revised: December 28, 2007
Published online: February 28, 2008

Keywords: fluorescence · luminescence · photoactivation · silver · zeolites

[1] a) T. Baba, Y. Iwase, K. Inazu, D. Masih, A. Matsumoto, *Microporous Mesoporous Mater.* **2007**, *101*, 142; b) J. A. Martens, A. Cauvel, A. Francis, C. Hermans, F. Jayat, M. Remy, M. Keung, J. Lievens, P. A. Jacobs, *Angew. Chem.* **1998**, *110*, 2003; *Angew. Chem. Int. Ed.* **1998**, *37*, 1901.
[2] T. Vosch, Y. Antoku, J. C. Hsiang, C. I. Richards, J. I. Gonzalez, R. M. Dickson, *Proc. Natl. Acad. Sci. USA* **2007**, *104*, 12616.
[3] a) S. Fedrigo, W. Harbich, J. Buttet, *J. Chem. Phys.* **1993**, *99*, 5712; b) C. Félix, C. Sieber, W. Harbich, J. Buttet, I. Rabin, W. Schulze, G. Ertl, *Chem. Phys. Lett.* **1999**, *313*, 105; c) G. A. Ozin, H. Huber, *Inorg. Chem.* **1978**, *17*, 155; d) W. Schulze, I. Rabin, G. Ertl, *ChemPhysChem* **2004**, *5*, 403.
[4] A. Henglein, *Chem. Rev.* **1989**, *89*, 1861.
[5] P. Mulvaney, A. Henglein, *J. Phys. Chem.* **1990**, *94*, 4182.
[6] J. T. Petty, J. Zheng, N. V. Hud, R. M. Dickson, *J. Am. Chem. Soc.* **2004**, *126*, 5207.
[7] J. Yu, S. A. Patel, R. M. Dickson, *Angew. Chem.* **2007**, *119*, 2074; *Angew. Chem. Int. Ed.* **2007**, *46*, 2028.
[8] N. Keghouche, M. Mostafavi, M. O. Delcourt, *J. Chim. Phys. Phys.-Chim. Biol.* **1991**, *88*, 855.
[9] P. A. Jacobs, J. B. Uytterhoeven, *J. Chem. Soc. Faraday Trans. 1* **1979**, *75*, 56.
[10] G. A. Ozin, F. Hugues, *J. Phys. Chem.* **1983**, *87*, 94.
[11] R. Seifert, R. Rytz, G. Calzaferri, *J. Phys. Chem. A* **2000**, *104*, 7473.
[12] G. Schulz-Ekloff in *Comprehensive Supramolecular Chemistry*, *Vol. 7* (Eds.: B. Alberti, T. Bein), 1st ed., Pergamon, Oxford, **1996**, p. 549.
[13] L. A. Peyser, A. E. Vinson, A. P. Bartko, R. M. Dickson, *Science* **2001**, *291*, 103.
[14] T. Sun, K. Seff, *Chem. Rev.* **1994**, *94*, 857.
[15] a) M. C. Kanan, S. M. Kanan, H. H. Patterson, *Res. Chem. Intermed.* **2003**, *29*, 691; b) S. M. Kanan, M. C. Kanan, H. H. Patterson, *J. Phys. Chem. B* **2001**, *105*, 7508; c) S. M. Kanan, M. C. Kanan, H. H. Patterson, *Curr. Opin. Solid State Mater. Sci.* **2003**, *7*, 443.
[16] G. Calzaferri, C. Leiggener, S. Glaus, D. Schurch, K. Kuge, *Chem. Soc. Rev.* **2003**, *32*, 29.
[17] R. Seifert, A. Kunzmann, G. Calzaferri, *Angew. Chem.* **1998**, *110*, 1603; *Angew. Chem. Int. Ed.* **1998**, *37*, 1521.
[18] R. Verberk, A. M. van Oijen, M. Orrit, *Phys. Rev. B* **2002**, *66*, 233202.
[19] R. A. Schoonheydt, H. Leeman, *J. Phys. Chem.* **1989**, *93*, 2048.
[20] L. A. Capadona, PhD Thesis, Georgia Institute of Technology, Atlanta, **2004**.
[21] S. Hashimoto, S. Yamashita, *ChemPhysChem* **2004**, *5*, 1585.
[22] a) M. B. J. Roeffaers, G. De Cremer, H. Uji-i, B. Muls, B. F. Sels, P. A. Jacobs, F. C. De Schryver, D. E. De Vos, J. Hofkens, *Proc. Natl. Acad. Sci. USA* **2007**, *104*, 12603; b) M. B. J. Roeffaers, J. Hofkens, G. De Cremer, F. C. De Schryver, P. A. Jacobs, D. E. De Vos, B. E. Sels, *Catal. Today* **2007**, *126*, 44; c) M. B. J. Roeffaers, B. F. Sels, H. Uji-i, B. Blanpain, P. L'Hoest, P. A. Jacobs, F. C. De Schryver, J. Hofkens, D. E. De Vos, *Angew. Chem.* **2007**, *119*, 1736; *Angew. Chem. Int. Ed.* **2007**, *46*, 1706.
[23] This program was developed in a cooperation between the Management of Technology Institute (Belarusian State University) and the Division of Photochemistry and Spectroscopy (Katholieke University of Leuven).

